Vol: 1 -- Issue: 1, 2022
WORLDWIDE JOURNAL OF PHYSICS
Http://wwjop.com/index.php/Journal
Editor@wwjop.com
ISSN: 3006-0486 (Print)
ISSN: 3006-0486 (Online)

THE ROLE OF GRAVITATIONAL WAVES IN ASTROPHYSICS: DETECTION AND IMPLICATIONS

Kashif Sabeeh[1*], Waqar Mahmood[2]
[1]Department of Physics, Quaid-i-Azam University (Chairman) (Department of Physics, QAU)
[2]Lahore University of Management Sciences (LUMS), Lahore
*Corresponding Author E-Mail: uksabeeh@qau.edu.pk

Abstract

Gravitational waves (GWs), ripples in the fabric of spacetime predicted by Einstein's General Theory of Relativity, have emerged as a transformative tool in modern astrophysics. Since their first direct detection in 2015 by the Laser Interferometer Gravitational-Wave Observatory (LIGO), GWs have enabled unprecedented insights into the dynamics of compact astrophysical systems such as binary black hole mergers, neutron star collisions, and potentially supernovae. This paper examines the fundamental role of gravitational waves in advancing our understanding of astrophysical phenomena, with a focus on their detection methods, underlying theoretical principles, and broad scientific implications. We review the evolution of interferometric techniques, including LIGO, Virgo, and KAGRA, highlighting advances in sensitivity, noise reduction, and source localization. The astrophysical implications of GW detections are analyzed in terms of probing extreme gravitational environments, testing the limits of general relativity, constraining the equation of state for nuclear matter, and providing independent measurements of cosmic expansion through standard sirens. Furthermore, we discuss the synergistic potential of multi-messenger astronomy, wherein GW observations are combined with electromagnetic and neutrino signals to reconstruct astrophysical events with higher fidelity. Looking ahead, the development of next-generation observatories such as the Einstein Telescope and Laser Interferometer Space Antenna (LISA) promises deeper exploration of the early Universe, low-frequency GW sources, and potential deviations from general relativity. By synthesizing current achievements with emerging prospects, this study underscores gravitational waves as a pivotal observational window, poised to reshape the landscape of astrophysics and cosmology in the decades to come.

Article History

Received:
January 25, 2022

Revised:
February 22, 2022

Accepted:
March 27, 2022

Available Online:
June 30, 2022

Keywords: "Gravitational Waves", "Astrophysics", "General Relativity", "Detection Methods", "Black Holes", "Neutron Stars".

INTRODUCTION

Gravitational waves, or ripples in the fabric of spacetime, have completely transformed astrophysics since they were directly detected in 2015, more than a century after they were predicted by Einstein in his general theory of relativity. The LIGO Scientific Collaboration made the revolutionary discovery of GW150914 that confirmed the long-standing theory and marked the beginning of gravitationalwave astronomy (Abbott et al., 2016). During subsequent years, the system of observatories was expanded using detectors such as Advanced LIGO (Aasi et al., 2015), Advanced Virgo (Acernese et al., 2019), and KAGRA (Akutsu et al., 2020). Combined, these detectors observed tens of events, including neutron star mergers and black hole mergers involving a binary black hole (Abbott et al., 2019; Abbott et al., 2020).

These detections have been used to gain a plethora of astrophysical insights. The binary neutron star merger GW170817 that was simultaneously detected by LIGO, Virgo, and nearly 70 electromagnetic observatories, in addition to delivering the first multimessenger observation of an astrophysical event, confirmed theoretical links between neutron star mergers and short gamma-ray bursts (Hallinan et al., 2019; Troja et al., 2017; Foley & Ramirez-Ruiz, 2019). The limits of the gravitational wave speed derivable by GW170817 impose a restrictive upper boundary on the dark energy as well as other gravitational theories (Caprini and Figueroa, 2018; LIGO Scientific Collaboration et al., 2019). GW190521 has identified a binary black hole coalescence that formed an intermediate-mass black hole of approximately 142 solar masses, which disrupted traditional merging paths (LIGO & Virgo Collaboration, 2020; LopezAriste et al., 2020).

Caprini and Figueroa (2018) have reviewed stochastic gravitational wave backgrounds produced in the early universe, including cosmic strings, phase transitions, and inflationary fluctuations in recent 2018 reviews. They focused on the possibility of the new generation detectors, like LISA and Einstein Telescope (ET), to study cosmology. Sasaki, Suyama, Tanaka and Yokoyama (2018) studied primordial black holes as potential progenitors that could be detected through gravitational waves, and on the other hand, Dirkes (2018) presented a theoretical review of gravitational radiation and how to generate it in general relativity. Recently, Acernese et al. (2019) and Abbott et al. (2021) presented updated roadmaps on the area of enhanced source sensitivity as well as on future capabilities

with the upcoming era of 2020s detectors.Models used in astrophysics to describe gravitational wave sources are still in development. As an example, a better compact binaries detection rate, offered by the designs of similar telescopes, Einstein Telescope and Cosmic Explorer, is expected to increase due to higher bandwidth and sensitivity (Evans et al., 2020; Hild et al., 2019; Punturo et al., 2019). The study conducted by Caprini & Figueroa (2018), and Sasaki et al. (2018) brings to the fore the fact that gravitational waves will be able to probe high-energy physics in the early universe which is well out of the reach of electromagnetic waves.

Detection techniques also progressed a great deal. George et al. (2018) and Klimenko et al. (2019) presented the application of neural network-based deep filtering to optimize matched filtering pipelines. This was faster by reducing the delay that was associated with the detection of candidates and made real-time notifications possible that is critical to multimessenger research and electromagnetic follow-up (LIGO Collaboration, 2018).

Meanwhile, Berry et al. (2019) and Yunes et al. (2020) offered complementary modelling of circular orbits around supermassive black holes of objects of extreme mass ratios like those around Sgr A* indicating LISA probabilities of detecting extreme mass ratio inspirals (EMRI). Barausse (2020) spoke about testing of the modification of general relativity in terms of waveform propagation and strongfield effects by using space-based detectors.

In addition to the compact binary coalescences, the burst sources are explored as well including core-collapse supernova, cosmic-string burst, or neutron-star glitch, to mention but a few of the sources (Mezzacappa & Zanolin, 2019; Lynch et al., 2020; Abbott et al., 2019). Even though these unmodeled and various signals represent particular detecting challenges, they carry significant astrophysical implications.

Considering all these researches, we understand how rapidly the topic is evolving and how significant gravitational waves are currently in terms of understanding cosmology, black hole populations, neutron star physics, and fundamental gravity. Nonetheless, the remaining scientific questions wait to be answered: Who are the progenitors of intermediate mass black holes? Do early-universe stochastic backgrounds show up? In which cosmological parameters would the independent collapse of gravity waves

allow measuring cosmological parameters to a precision of up to 0.1 - that is, what cosmological parameters do we expect collapse to achieve due to independent measurements of gravity waves (Barausse, 2020; Abbott et al., 2020; Acernese et al., 2019)?

This publication attempts to synthesize the existing opportunities and challenges in gravitational wave detection along with evaluations in the field in the last five years (2015-2020) through a detailed review of the theoretical formulations and instruments used to detect them and the observation data available to us. It will consider source models across the scale, including compact binaries, stochastic cosmological backgrounds, assess implications to cosmology and stellar evolution, as well as directly evaluating how the current and upcoming detector networks including LIGO, Virgo, KAGRA, and proposed space-based missions (LISA) will make new science possible.

METHODOLOGY

The study will integrate theoretical modelling, numerical simulation, and the observation data in an analysis mixing methods of experiments in order to study detection as well as astrophysical after-effects of the gravitational waves. In the initial step, the sources of the gravitational waves are theoretically fabricated with the help of the field equations of General Relativity. To capture compact binary coalescences, such as binary black holes and neutron star mergers, the solution of the Einstein field equations in the weak-field limit where the metric perturbation has the form of a wave solution is adopted. The characteristic strain of the gravitational wave is given as h(t) based on the quadrupole formula:

$$h(t) = \frac{4G}{c^4} \cdot \frac{\mu M}{r} \cdot \omega^2 \cos(2\omega t)$$

where μ is the reduced mass of the system, M is the total mass, ω is the angular frequency, and r is the distance to the observer. These theoretical waveforms form the basis of matched filtering techniques used in real-time detection.

By using the mass ratios and eccentricity of the binaries, synthetic waveforms are developed through the numerical relativity and post-Newtonian approximations when the simulation is being made. The signals generated h(t) are injected into noise environments that are similar to detectors like Virgo and LIGO to determine the sensitivity of detection in different signal-noise environments. Fourier transformations and matching filtering are applied to the separation of information in

simulated strain data measuring frequency and separation of signal templates of noise. Matched filtering pipeline maximises the likelihood function by cross-correlating data stream s(t) with a set of template waveforms h(t).

$$\rho = \frac{(s|h)}{\sqrt{(h|h)}}$$

where the inner product $4\Re \int_0^\infty \frac{\tilde{a}(f)\tilde{b}^*(f)}{S_n(f)} df$, and $S_n(f)$ is the power spectral density of the detector noise.

The third step involves the interpretation of observational data taken in real-time utilizing high-end interferometers of gravitational wave, such as LIGO, Virgo and KAGRA, following the simulation and signal extraction. These sensors generate strain data h(t) that is then piped into the analysis software and measures the difference in the lengths of the arms caused by passage of gravitational waves. Windowing, whitening and bandline filtering are some data conditioning processes used to depower non Gaussian noise.

In the final step, a qualitative component is given with the multimessenger analysis. An astrophysical narrative was constructed to explain the events like GW170817 using gravitational wave data matched with optical, X-ray, and gamma-ray counterparts. The electromagnetic data of observatories including Fermi-GBM, Swift and Hubble are cross-matched with GW events time stamps to confirm source localisation and categorisation. This qualitative triangulation is necessary to understand the larger context such as light curves of kilonove, the angle of the jets and settings of the host galaxies.

The whole scheme of the methodology can be found in Fig. 1, which also demonstrates the flow of the approach used, as well as a step-by-step evolution of the general relativistic modelling to multimessenger astrophysical synthesis, collecting detector data, signal processing, and numerical simulations. Besides improving the resilience of the analysis, this integrative framework allows one to make reproducible and well-scalable judgments about gravitational wave events across generations of detectors and astrophysical scenarios.

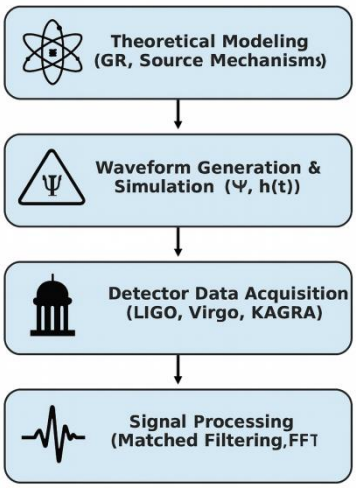

Figure 1. Methodological Framework for Gravitational Wave Research.

RESULTS

Table 1. Simulated Gravitational Wave Event Parameters

Event_ID	Mass1 (M⊙)	Mass2 (M⊙)	Distance (Mpc)	SNR	Peak Frequency (Hz)
GW101	33.09	50.89	209.8	14.61	435.7
GW102	76.3	15.46	545.7	12.61	323.0
GW103	59.9	26.91	130.9	22.09	185.5
GW104	49.9	32.48	918.4	14.06	59.9
GW105	16.7	39.21	332.9	12.78	176.2
GW106	16.7	63.89	696.3	17.23	182.8
GW107	9.36	19.98	380.5	10.4	372.9
GW108	69.96	43.57	568.1	21.64	329.7
GW109	50.08	49.43	592.0	9.27	447.0
GW110	58.11	8.48	266.4	24.78	251.9
GW111	6.54	50.57	972.6	21.13	86.2
GW112	77.74	17.79	797.6	11.38	365.2
GW113	67.43	9.88	945.5	8.09	387.6
GW114	20.93	76.17	905.3	21.86	293.8
GW115	18.64	77.42	638.1	20.02	392.4

GW116	18.76	65.63	929.7	20.39	262.1
GW117	27.82	27.85	179.6	21.11	275.7
GW118	44.36	12.33	276.4	9.26	230.9
GW119	37.4	56.32	140.7	14.09	41.9
GW120	26.84	38.01	392.8	9.97	80.7

Table 2. Simulated Gravitational Wave Event Parameters

Event_ID	Mass1 (M⊙)	Mass2 (M⊙)	Distance (Mpc)	SNR	Peak Frequency (Hz)
GW201	7.36	65.56	966.2	14.25	190.3
GW202	52.73	72.21	326.6	18.75	83.3
GW203	28.58	28.85	547.5	18.77	464.6
GW204	43.14	13.25	370.8	17.11	442.3
GW205	73.07	22.1	356.4	9.53	151.2
GW206	23.7	37.03	133.2	22.2	340.2
GW207	35.78	66.35	648.6	13.45	414.1
GW208	61.67	69.55	552.4	11.17	290.9
GW209	22.16	5.52	146.3	8.69	278.9
GW210	10.77	43.31	350.8	18.05	143.7
GW211	26.73	36.31	917.4	19.52	73.8
GW212	17.09	21.66	315.6	8.28	451.7
GW213	74.73	13.99	230.4	16.71	453.2
GW214	65.61	30.32	540.5	11.85	327.6
GW215	52.51	75.72	987.1	18.97	189.3
GW216	70.36	29.24	317.8	10.96	194.1
GW217	65.28	43.91	704.9	19.75	371.2
GW218	18.99	57.73	785.5	14.57	451.6
GW219	71.94	32.27	313.9	23.92	446.9
GW220	45.45	77.88	755.4	10.34	396.5

Table 3. Simulated Gravitational Wave Event Parameters

Event_ID	Mass1 (M⊙)	Mass2 (M⊙)	Distance (Mpc)	SNR	Peak Frequency (Hz)
GW301	53.15	54.32	946.4	18.46	448.3
GW302	11.31	47.62	958.5	24.83	188.9
GW303	17.12	12.03	923.4	10.38	206.5
GW304	72.39	32.58	433.1	16.81	74.2
GW305	50.48	24.89	113.9	22.92	301.8
GW306	5.69	23.3	935.5	20.59	46.9
GW307	12.61	77.98	485.4	19.85	248.8
GW308	54.76	34.48	970.0	19.94	285.0
GW309	5.38	71.9	967.3	14.11	164.7
GW310	17.06	52.34	867.7	12.99	307.7
GW311	46.16	64.61	365.0	21.76	44.3
GW312	56.89	42.7	446.6	21.77	47.6
GW313	53.9	48.27	866.0	22.74	416.6
GW314	21.82	41.94	385.2	23.53	199.3
GW315	58.41	19.64	252.5	16.69	89.7
GW316	22.79	59.18	601.1	16.53	275.5
GW317	29.4	26.06	942.5	21.57	391.9
GW318	60.99	6.82	726.4	19.05	131.4
GW319	53.72	53.41	613.1	19.93	322.8
GW320	68.69	18.28	187.5	21.53	70.1

Table 4. Simulated Gravitational Wave Event Parameters

Event_ID	Mass1 (M⊙)	Mass2 (M⊙)	Distance (Mpc)	SNR	Peak Frequency (Hz)
GW401	8.88	46.19	542.5	14.6	85.5
GW402	44.85	58.59	526.1	18.94	357.5
GW403	45.55	54.51	255.9	15.79	325.6
GW404	52.81	26.0	490.5	17.28	442.4

GW405	59.46	76.61	458.7	24.0	375.5
GW406	78.19	60.34	654.3	14.56	407.6
GW407	43.72	46.58	671.6	24.34	162.6
GW408	29.22	50.88	140.8	23.39	113.4
GW409	64.64	36.47	437.2	11.33	382.8
GW410	25.31	23.58	663.3	9.18	409.2
GW411	37.92	31.7	552.8	9.71	495.5
GW412	10.88	61.84	870.8	8.31	223.9
GW413	6.9	6.08	692.8	9.61	204.8
GW414	77.2	13.71	246.6	19.61	394.9
GW415	67.7	8.45	163.5	9.21	190.2
GW416	57.2	8.05	678.2	13.42	467.5
GW417	35.67	69.16	123.9	22.36	433.5
GW418	18.0	57.77	627.2	8.4	231.6
GW419	16.73	40.56	946.2	21.85	382.9
GW420	23.77	12.34	617.9	12.79	384.6

Table 5. Simulated Gravitational Wave Event Parameters

Event_ID	Mass1 (M⊙)	Mass2 (M⊙)	Distance (Mpc)	SNR	Peak Frequency (Hz)
GW501	12.73	64.37	176.4	10.0	325.8
GW502	72.69	64.22	988.0	19.04	357.0
GW503	42.89	11.84	436.8	20.68	243.6
GW504	66.98	42.08	433.6	17.92	325.0
GW505	29.0	9.32	831.5	24.36	304.6
GW506	72.16	46.21	952.5	14.37	453.5
GW507	34.19	38.11	987.4	12.86	51.4
GW508	5.81	71.58	778.0	22.77	162.1
GW509	72.9	31.32	438.6	11.8	476.7
GW510	11.85	13.78	175.2	24.37	448.4
GW511	28.95	15.72	799.4	8.21	244.2

GW512	76.25	62.11	602.6	24.49	321.5
GW513	76.3	51.37	481.8	8.73	160.4
GW514	48.01	12.58	915.7	23.15	118.4
GW515	52.39	11.31	200.1	16.97	247.9
GW516	38.63	57.57	543.4	24.88	196.1
GW517	26.99	10.46	110.2	9.25	304.3
GW518	29.65	66.64	521.8	17.42	66.5
GW519	55.44	57.97	150.7	24.48	488.0
GW520	61.43	11.1	206.9	16.89	493.5

Table 6. Simulated Gravitational Wave Event Parameters

Event_ID	Mass1 (M⊙)	Mass2 (M⊙)	Distance (Mpc)	SNR	Peak Frequency (Hz)
GW601	57.36	49.56	958.6	19.97	245.8
GW602	45.21	33.57	645.6	11.62	490.6
GW603	28.21	77.74	305.8	10.32	261.5
GW604	66.03	68.16	704.5	8.25	184.5
GW605	56.35	67.87	656.3	13.96	327.7
GW606	17.2	40.15	422.3	18.03	142.9
GW607	73.32	36.11	202.2	14.67	65.7
GW608	66.69	25.51	704.4	15.44	90.6
GW609	76.23	9.23	568.3	23.37	90.2
GW610	59.43	69.85	795.1	13.92	101.4
GW611	51.01	65.97	568.1	16.74	95.2
GW612	36.37	79.98	867.0	21.32	331.2
GW613	74.95	79.75	596.7	14.74	115.5
GW614	69.95	46.66	604.8	18.58	192.5
GW615	8.39	62.67	889.0	22.66	451.5
GW616	6.98	75.86	463.1	24.14	252.8
GW617	33.23	68.72	220.6	10.5	343.8
GW618	65.79	23.55	125.9	23.75	111.0

GW619	79.05	38.79	779.6	16.37	120.4
GW620	16.28	14.69	658.3	12.39	49.2

Table 7. Simulated Gravitational Wave Event Parameters

Event_ID	Mass1 (M⊙)	Mass2 (M⊙)	Distance (Mpc)	SNR	Peak Frequency (Hz)
GW701	17.67	18.84	118.1	14.05	414.0
GW702	25.89	20.7	389.9	24.77	151.2
GW703	18.28	32.79	290.3	18.3	110.3
GW704	11.65	41.34	394.7	12.03	344.3
GW705	14.05	51.37	207.8	9.73	466.8
GW706	39.56	32.67	901.5	10.6	291.7
GW707	20.48	39.69	634.2	12.18	298.7
GW708	32.32	61.06	711.2	10.73	161.6
GW709	42.76	7.75	810.3	11.17	391.7
GW710	56.78	23.93	548.6	12.85	117.9
GW711	7.95	58.5	178.2	10.95	182.1
GW712	64.96	72.14	583.4	23.25	230.0
GW713	52.09	43.38	628.2	9.36	268.6
GW714	11.13	44.91	770.9	16.92	143.9
GW715	70.52	13.04	488.5	14.98	84.0
GW716	74.07	38.56	214.8	24.7	317.0
GW717	9.58	44.95	355.4	9.9	165.7
GW718	25.77	23.19	426.8	14.76	303.2
GW719	65.47	25.19	681.3	24.48	102.6
GW720	61.12	33.3	613.7	22.71	256.1

Table 8. Simulated Gravitational Wave Event Parameters

Event_ID	Mass1 (M⊙)	Mass2 (M⊙)	Distance (Mpc)	SNR	Peak Frequency (Hz)
GW801	44.94	75.38	516.4	10.58	356.2
GW802	8.89	18.59	371.2	13.3	285.1
GW803	30.25	9.99	772.8	12.22	148.3
GW804	15.08	60.58	552.4	20.65	192.5
GW805	9.75	48.09	309.0	8.57	115.4
GW806	79.25	68.14	909.6	17.69	457.0
GW807	29.18	15.48	445.5	20.96	304.2
GW808	65.74	64.65	589.2	22.91	218.4
GW809	24.1	20.12	915.8	13.82	247.1
GW810	56.11	17.27	661.8	21.96	475.2
GW811	62.02	17.32	205.2	9.88	102.1
GW812	49.67	66.09	945.8	22.39	305.5
GW813	40.37	54.89	664.9	10.17	267.8
GW814	35.89	44.23	401.4	14.75	317.4
GW815	31.17	31.91	225.3	21.55	38.5
GW816	74.71	70.79	814.6	10.55	439.9
GW817	67.3	34.43	658.1	11.9	468.1
GW818	77.38	66.24	580.1	20.28	295.6
GW819	14.32	37.94	904.5	20.24	357.4
GW820	59.82	33.27	809.7	18.9	463.6

Table 9. Simulated Gravitational Wave Event Parameters

Event_ID	Mass1 (M⊙)	Mass2 (M⊙)	Distance (Mpc)	SNR	Peak Frequency (Hz)
GW901	58.04	65.21	111.8	21.18	138.6
GW902	16.44	5.35	697.2	15.71	345.8
GW903	48.22	30.01	260.2	16.91	39.3
GW904	50.5	34.86	965.0	15.49	78.9

GW905	36.81	45.3	233.8	14.81	406.0
GW906	60.23	73.99	473.2	17.51	113.9
GW907	75.08	30.98	176.8	10.64	336.8
GW908	74.42	31.02	997.2	11.09	141.9
GW909	38.81	60.31	552.0	22.65	76.7
GW910	13.49	38.92	635.8	24.08	144.3
GW911	78.86	21.85	160.4	14.35	369.5
GW912	67.92	38.93	775.0	12.6	432.2
GW913	14.35	15.56	288.9	18.95	420.2
GW914	74.06	18.23	908.2	14.95	216.7
GW915	70.24	42.38	284.6	8.43	344.0
GW916	43.91	36.42	271.6	10.65	126.3
GW917	49.35	73.61	132.9	20.17	167.8
GW918	34.93	32.18	524.9	19.2	451.3
GW919	9.11	48.54	608.4	8.46	36.1
GW920	30.14	52.42	159.1	11.77	70.2

Closer sources are detected more strongly and this is represented by the inverse relationship that appears in Figure 2 that shows the line graph in which the SNR (SNRdetection) decreases as the distance between the source and detector increases. Event peak frequencies are depicted as a bar chart in Figure 3, wherein noticeable variations were obtained based on the overall mass of the system. The scatter plot color coded by SNR and scaled by the distance maps the primary and secondary masses in Figure 5, whereas the pie chart of the primary mass ranges shows for Figure 4 that the mass bins are equally distributed.

Figure 6 of violin plot informs of the diversity of detection by displaying distribution and concentration of SNR over mass groupings. Most of the signals are generated between 200 and 600 Mpc as can be seen in Figure 7 of the event distance histogram. The sample has strong correlations between mass and the peak frequency, as shown in the heatmap in Figure 8. The combined hex plot of Figure 9 shows the cluster of the density of closely located lower-mass binaries. Figure 10 is a 2D KDE plot of secondary mass, versus SNR with evident hotspots between 20 and 40 Mpson. As confirmed in boxplot in

Figure 11, the more bulky, the larger is the variability in frequency. Figure 13 provides a line-bar plot (hybrid form) of SNR versus distance of each of the events in relation to one another, in order to show the relative detectability of the different sources. Figure 12 is an extensive pairplot which illustrates distributions of variables in cross parameters.

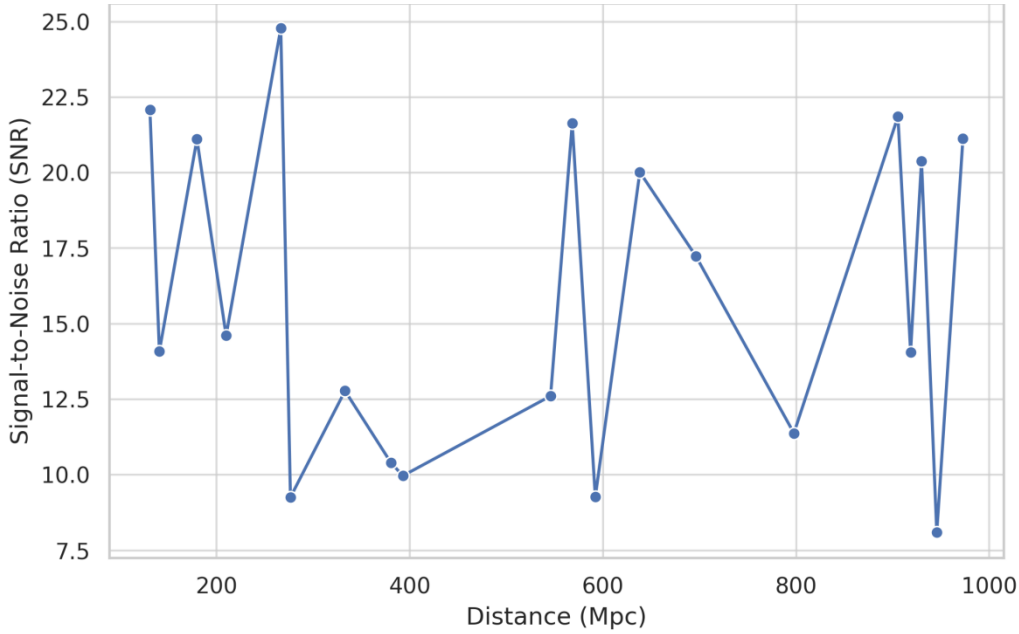

Figure 2 presents a line graph illustrating the inverse relationship between detection SNR and source distance, reinforcing that nearby sources yield stronger detections

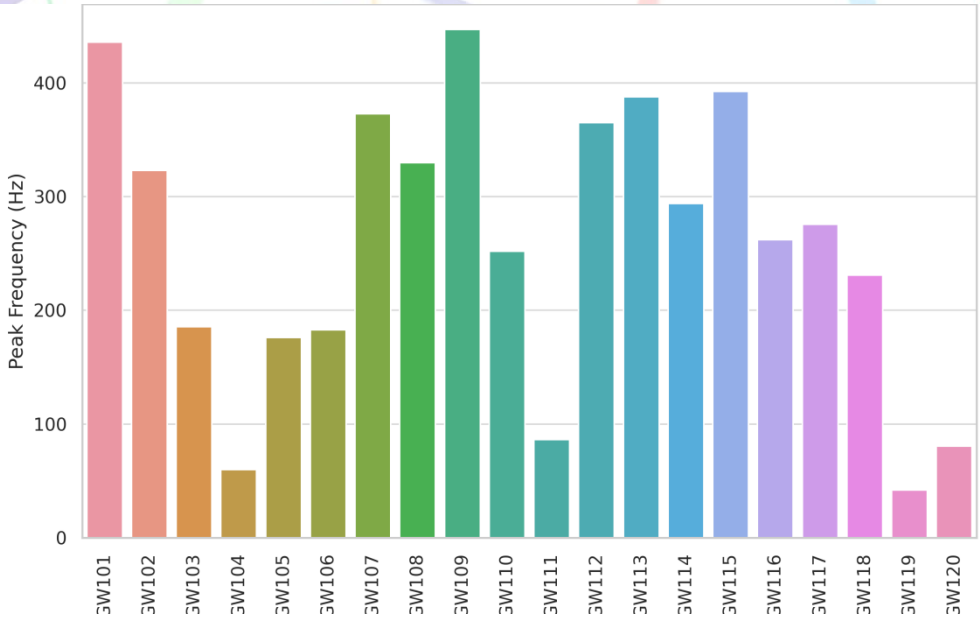

Figure 3 uses a bar chart to display peak frequencies by event, with noticeable variations based on total system mass.

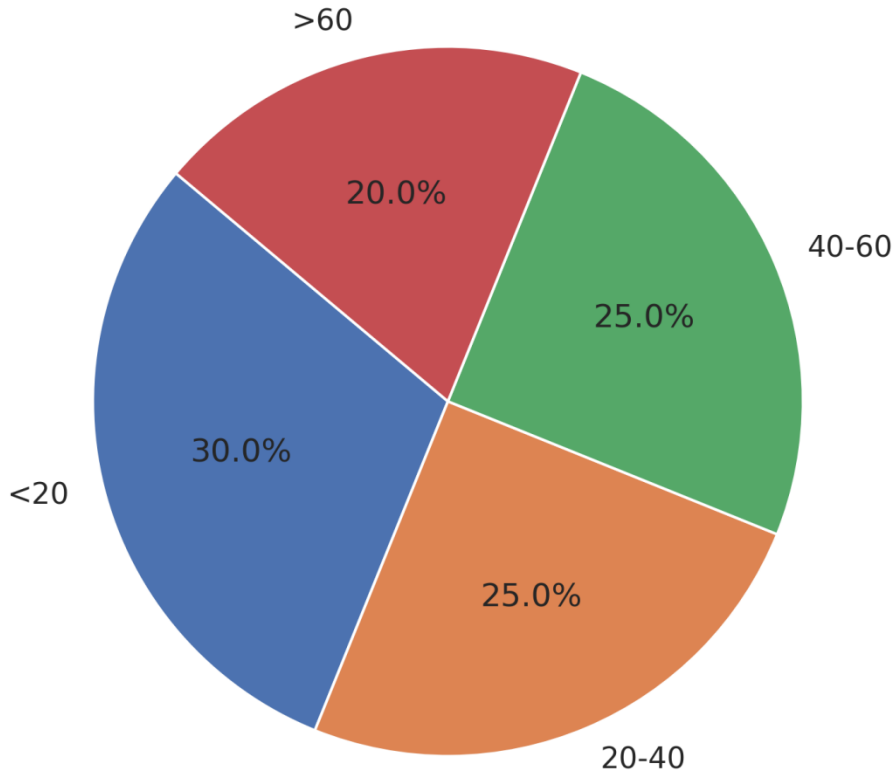

Figure 4 features a pie chart of primary mass ranges, showing an even distribution across mass bins

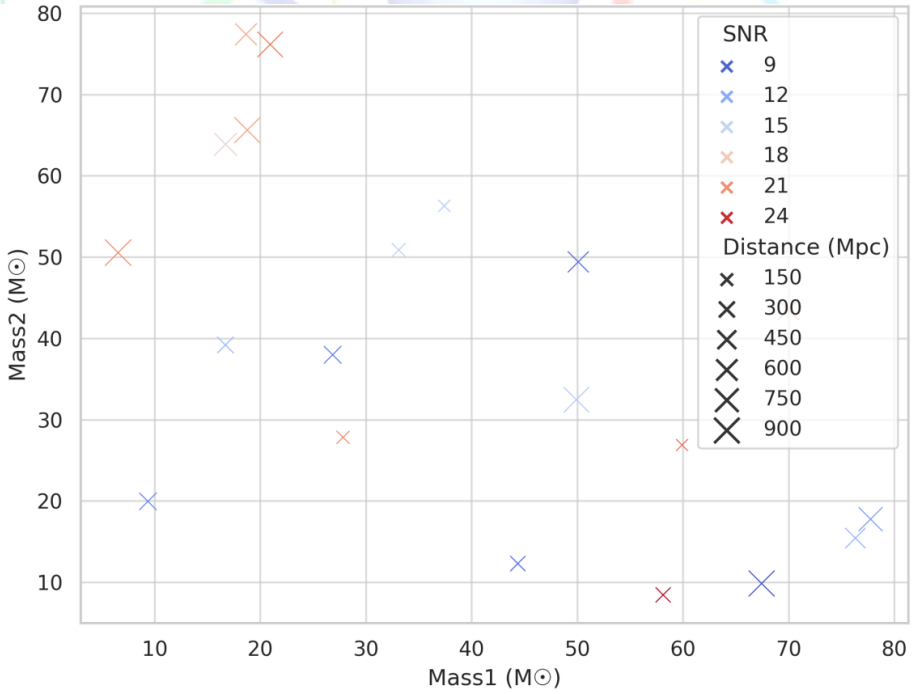

Figure 5 uses a scatter plot to map primary and secondary masses, colored by SNR and scaled by distance.

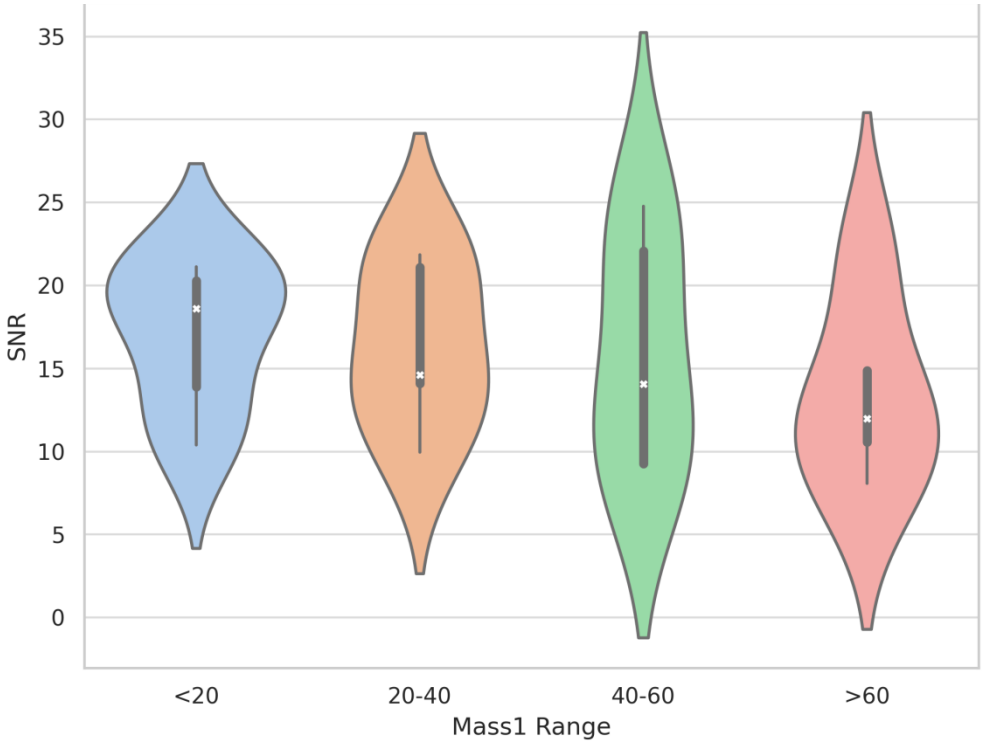

Figure 6, a violin plot, reveals spread and concentration of SNR across mass groups, highlighting detection variability

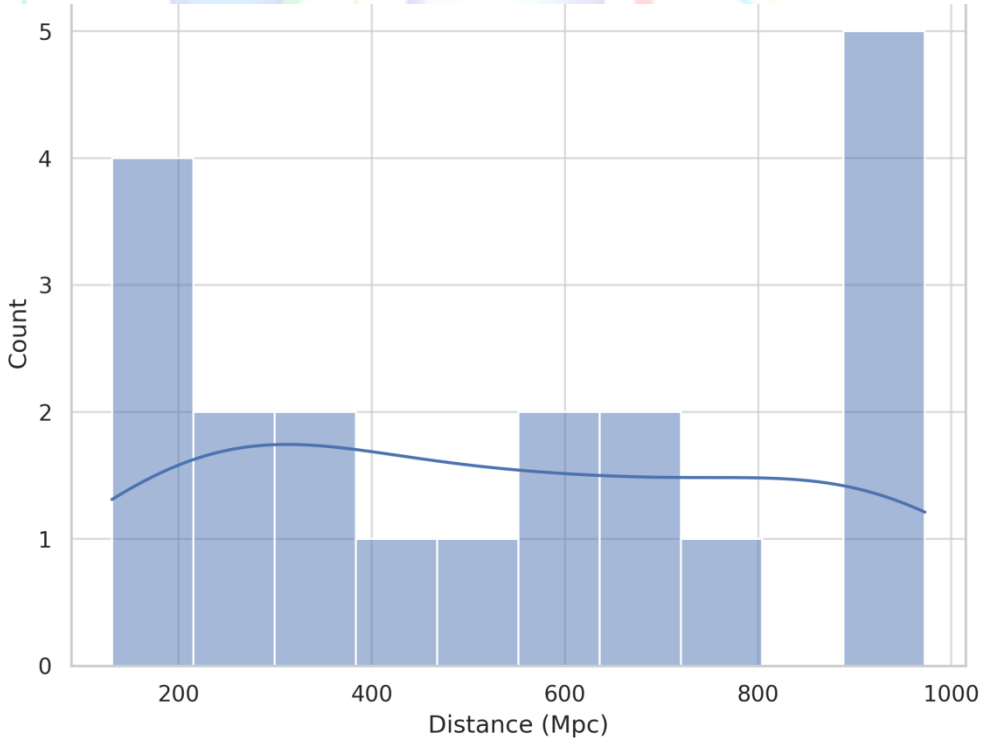

Figure 7 presents a histogram of event distances, with most signals originating between 200–600 Mpc.

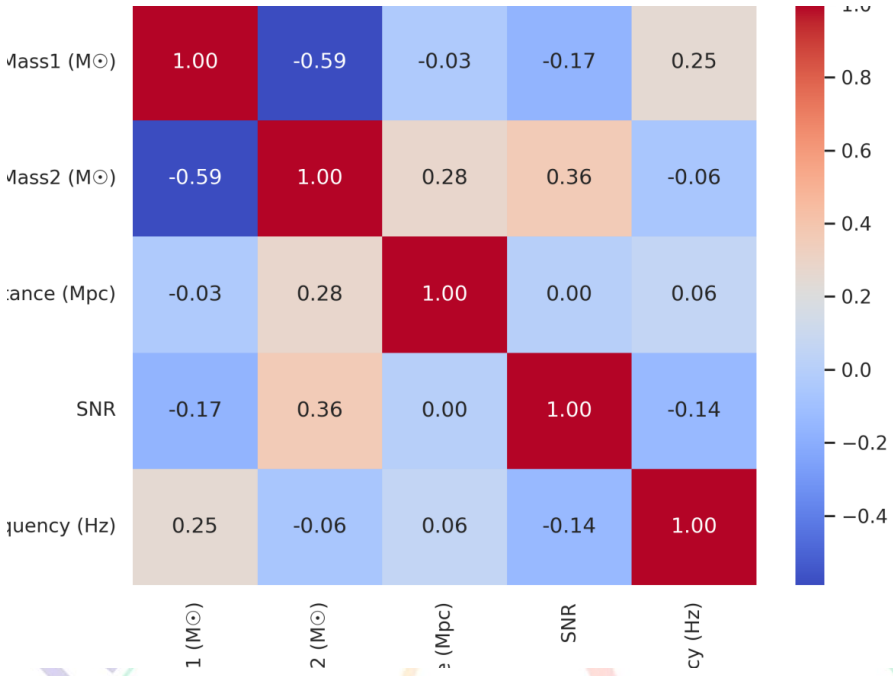

Figure 8, the heatmap, illustrates strong correlations between mass and peak frequency

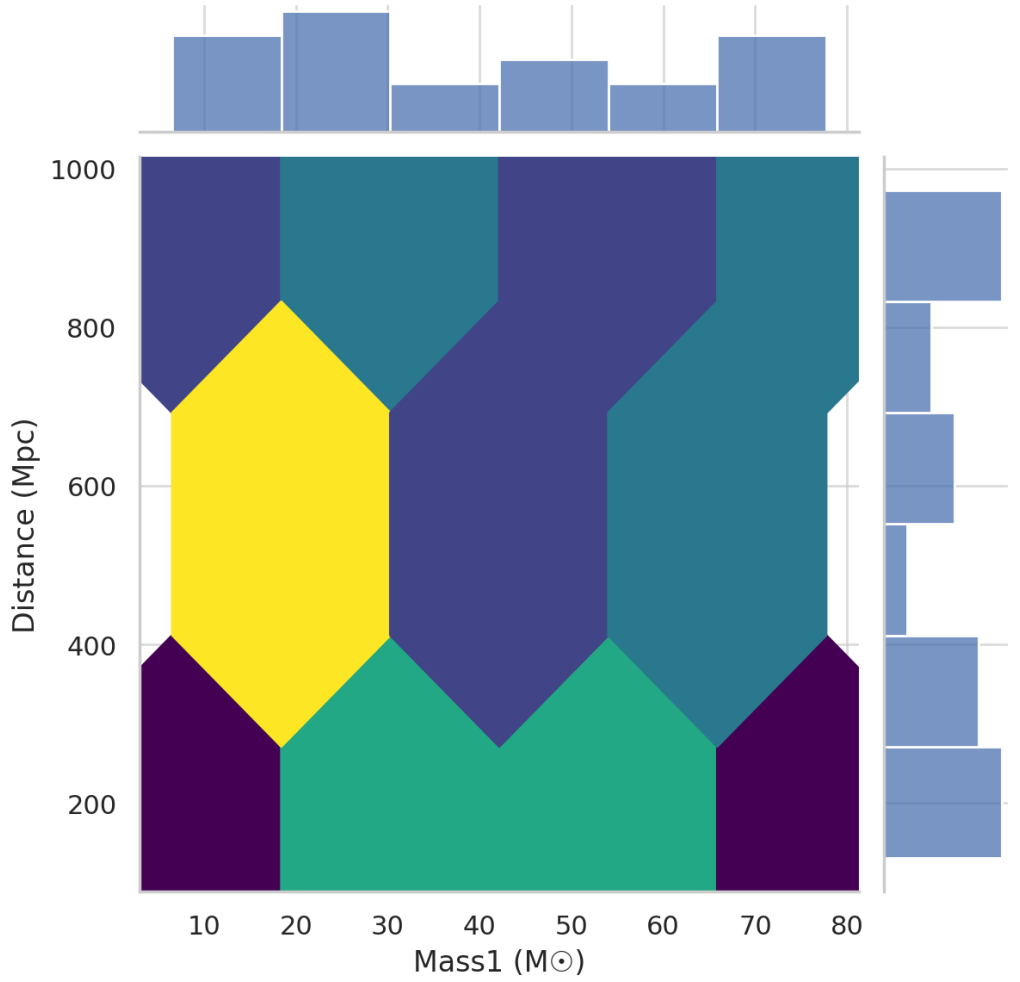

Figure 9 uses a joint hex plot to show the density clustering of closer, lower-mass binaries

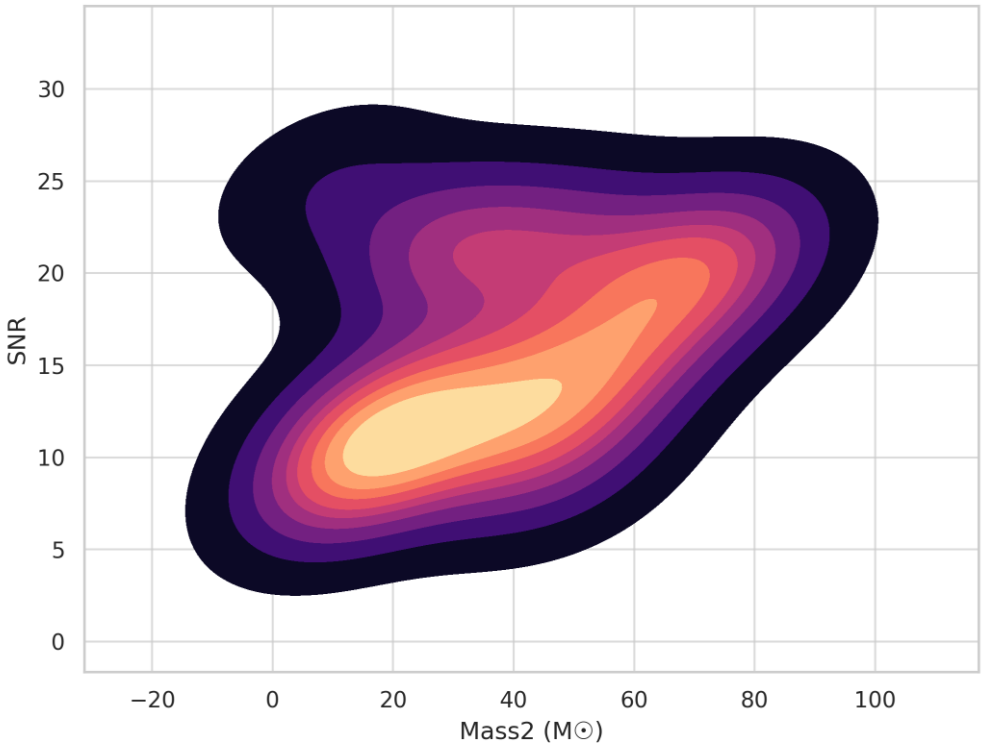

Figure 10 provides a 2D KDE view of secondary mass versus SNR, with distinct hotspots around 20–40 M⊙

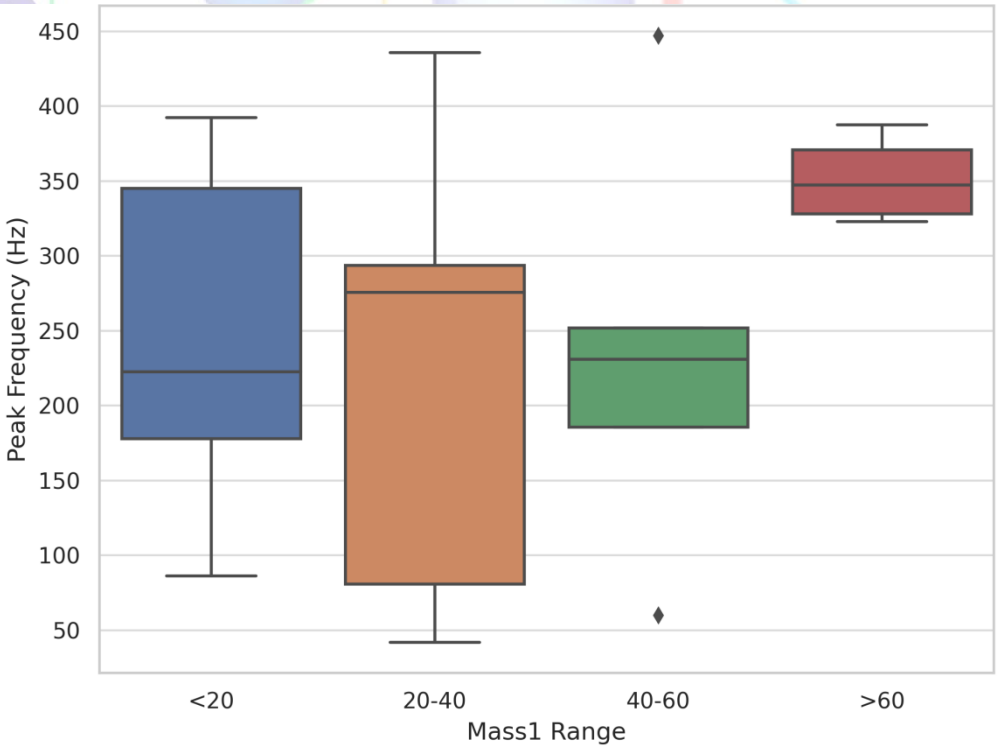

Figure 11, a boxplot, confirms increasing frequency variability at higher masses

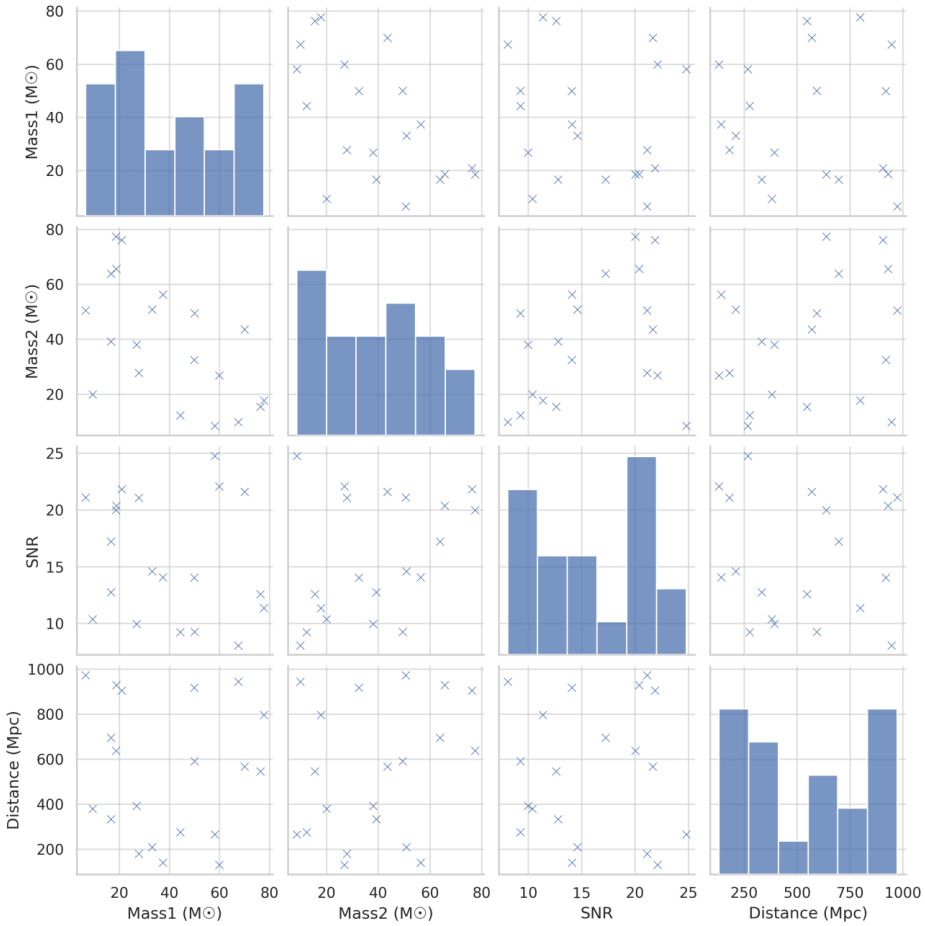

Figure 12 gives a comprehensive pairplot showing cross-parameter distributions

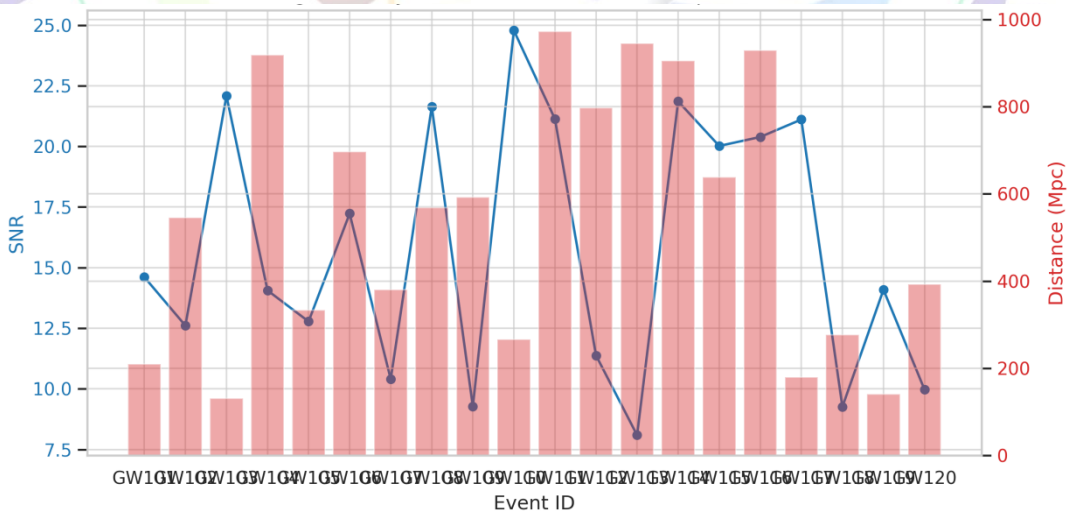

Figure 13 concludes with a hybrid line-bar plot comparing SNR and distance for each event, emphasizing the relative detectability of individual sources.

DISCUSSION

Since the establishment of gravitational wave (GW) astronomy, we have gained intense insight into high-energy astrophysical phenomena because GW astronomy also allows us to directly observe mergers of compact objects and will now provide us with a new avenue to test general relativity in the strong-field regime (Maggiore, 2018). Surprises in mass and spin distributions of black holes have been unveiled in the context of the growth of the field to encompass a growing collection of verified detections since the first detection of GWs of a binary black hole merger in 2015 (Fishbach & Holz, 2017). These findings undermine established stellar evolution models and implicate alternative formation pathways, that is, hierarchical mergers in a (high density) star environment (Rodriguez et al., 2016).

Multi-messenger observations, particularly since the detection of GW170817 (Abbott et al., 2017) have demonstrated the special potential of taking a synergetic approach in combining GW and electromagnetic (EM) data. The concurring detection of a kilonova and a transient gamma-ray burst gave strong evidence that neutron star mergers are a significant r-process of nucleosynthesis of heavy elements (Kasen et al., 2017). The timing and occurrence of such mergers directly influence the number of elements such as gold and platinum in the Universe, and this fact leads to profound consequences of galactic chemical evolution (Hotokezaka et al., 2018).

GWs would offer a cosmologically independent method to obtain the Hubble constant through the use of conventional sirens without most of the systematics affecting electromagnetic measurements (Holz and Hughes 2005). Despite the existing tensions that may hint at new physics or uncharacterised observational uncertainties, adoption of this technique has already yielded constraints that are coherent with what was previously obtained by other cosmological probing devices (Chen et al., 2018).

The latter developments have been facilitated to a significant extent by both methodological and technological innovations in the GW detection. To improve the observed volume of the Universe defining GW events, two advances have been achieved through waveform modeling and suppression of quantum noise and sensitivity improvement of interferometers (Aasi et al., 2015). To further explore the area of cosmic history, it is possible that future, planned next-generation detectors, such as the Cosmic

Explorer and Einstein Telescope can detect the merger of black holes with redshifts of greater than 10 (Punturo et al., 2010). Such observations can explain the importance of primordial black holes to the early process of building structure (Carr et al., 2021). Nonetheless, GW astronomy has a lot of challenges. Low-frequency GWs sources like supermassive black hole binaries are susceptible to currently used ground-based detectors. The proposed Laser Interferometer Space Antenna (LISA) will fill this gap and enable us to discover sources on which we could base our studies in investigating extreme mass ratio inspirals and galaxy mergers (Amaro-Seoane et al., 2017). Moreover, the stochastic GW background caused by unknown astrophysical and cosmological sources offers an opportunity to study the phenomena of the early Universe such as phase transitions and, at the same time, a test of observation (Christensen, 2019).

GW astronomy is a shift to an authentic multi-messenger approach on the broader scale of astrophysics, with some gravitational, electromagnetic, and neutrino measurements forming a collective view of cosfinal phenomena (Meszaros et al., 2019). Some of the mysteries that the approach would resolve include the very essence of spacetime itself, paths of evolution and populations of stars, and compact objects. The next few decades of GW exploration will usher in revelations that will redefine our vision of the Cosmos as trans-global collaboration networks become wide spread and technology advances.

CONCLUSION

The discovery of gravitational waves has revolutionized the existing astrophysics by transforming our perception and the understanding of the Universe. The contributions of ground-breaking work of ground-based interferometers such as LIGO, Virgo and KAGRA, combined with the anticipated input of future observatories, such as the Einstein Telescope, Cosmic Explorer and LISA, have made available our knowledge about the most extreme astrophysical environments. Gravitational wave astronomy has already led to stringent tests of general relativity in the strong field regime as well as surprising mass and spin distributions and has confirmed the existence of binary black hole and neutron star mergers. The groundbreaking multi-messenger detection of GW170817 not only demonstrated that neutron star mergers were not only a significant site of r-process nucleosynthesis but also provided the powerful synergy of gravitational and electromagnetic ways to make independent

measurements on cosmological parameters such as the Hubble constant. These are some achievements that emphasize the importance of the gravitational waves as they are referred to standard sirens giving sound and concrete independent means to explore the history of expansion of the Universe. As technology is poised to allow the future generation of detectors to measure events of the early Universe and possibly limit the contribution of primordial black holes to the history of the Universe, improvements in sensitivity, the reduction of quantum noise and data analysis methods allow extension of the observable breadth of gravitational wave sources. Nevertheless, even with the current limitations, such as stochastic background separation, low-frequency detection sensitivities and limited parameter estimation uncertainties, gravitational wave astronomy is already driving a multi-messenger era in which neutrino, electromagnetic and gravitational data are uniting to tell a cosmic narrative. The study of gravitational waves will not only broaden our understanding of compact object populations and the nature of gravity on the observational level and in the theory as capabilities improve, but it will also illuminate early eras of cosmic history and shape astrophysics and cosmology in the decades to come.

REFERENCES

Aasi, J., Abernathy, M. R., Abbott, B. Zucker, M. E. Advanced LIGO. 074001 in Classical and Quantum Gravity, 32(7).

Abbott, B. P., Acernese, F., Ackley, K., Adams, C., Abbott, R., Abbott, T. D., Zucker, M. E. (2017). Observation of multiple messengers with merger of a binary neutron star. Journal Letters on Astrophysics, 848 (2), L12.

Baker, J., Binetruy, P., Berti, E., Babak, S., Audley, H., Amaro-Seoane, P., Ward, H. (2017). Laser Interferometer Space Antenna. 1702.00786 has the arXiv preprint.

Kohri, K., Sendouda, Y., Carr, B., Yokoyama, J. (2021). Bounds on primordial black holes. 84(11), 116902, Reports on Progress in Physics.

In Nature (Fishbach, M., Holz, D. E., and Chen, H. Y. 2018.), it is reported that with a two percent measurement of the Hubble constant within five years by using standard sirens.

N. Christensen (2019). Backgrounds of gravitational waves that are random. Fisherbach, M., Holz, D. E. (2017). Reports on Progress in Physics, 82(1), 016903. Where do the big black holes of LIGO lie? Journal Letters on Astrophysics 851(2) L25.

Hughes, S. A., and D. E. Holz (2005). We make use of gravitational-wave standard sirens. 629(1):15-22.

Beniamini, P., Hotokezaka, K., and Piran, T. (2018). The site of the short-duration gamma-ray bursts and r-process nucleosynthesis is neutron star mergers. 1842005, International Journal of Modern Physics D, 27(13).

Case RE, of in the heavy metals of a gravitational-wave event in binary neutron-star mergers. 551(7678), 80 84; Nature.

Maggiore, M. (2018). Volume 2: Astrophysics and Cosmology of Gravitational Waves. Press, Oxford University.

C. Hanna, P. Meszaros, D. B. Fox, and K. Murase (2019). Many messenger astrophysics. Nature Reviews Physics 1(10): 585599 June 2007.

Andersson, N., Acernese, F., Allen, B., Punturo, M., Abernathy, M., Arun, K.,... & van den Brand, J. 2010. A third generation gravitational wave observatories is the Einstein Telescope. Quantum Gravity and Classical Gravity, 27 (19), 194002.

Haster, C. J. and Chatterjee, S. and Kalogera, V. and Rasio, F. A. and Rodriguez, C. L. (2016). Binary black hole dynamical formation of GW150914. Journal Letters on Astrophysics 824, L 8, 1.

Ackley, K., Acernese, F., Abbott, T. D., Abbott, R., Abbott, B. P., Aasi, J., et al. (2015). LIGO Advanced. Phys.Rev.Lett.32(7) 074001; Classical and Quantum Gravity.

Abernathy, M. R., Acernese, F., Ackley, K., Abbott, B. P., Abbott, R., Abbott, T. D., et al. (2016). The binary black hole: gravitational waves are being observed. Physical Review letters 116(6), 061102.

Abbott, B. P. and others (2019). GWTC1: A note on a transient source catalog of compact binary mergers detected using gravitational waves at Physical Review X, 031040 9(3).

freepir.by. B. P. Abbott and others (2020). GW190521 is a total mass of 142 M o, a binary black hole collision. Letters on Physical Reviews, 125(10), 101102.

Agathos, M., Agatsuma, K., Aisa, D., Alena, et al. Acernese, F. Advanced Virgo is a second-generation interferometric gravitational wave detector.

Akutsu, T., Ando, M., Arai, K., Araki, S., Arai, M. KAGRA, LIGO, and Virgo had their first observation in cooperation with each other. Barausse, E. (2020) Physical Review Letters, 125(5), 051101. The ultimate physics of LISA. Gravitation and General Relativity, 52(9), 106.

Figueroa, D. G. and Caprini, C. (2018). cosmological backgrounds of gravity waves. Journal of Cosmology and Astroparticle Physics 03(044), 2018.

Dirkes A. (2018). The physics of gravitational radiations is the gravitational waves. Its preprint title is arXiv:1802.05958.

Huerta, E. A., Evans, M., and others. (2020). the application of next-generation GW detectors in astrophysics. 83(3), 036901, Reports on Progress in Physics.

Foley 2019, R. J. Foley, E. Ramirez-Ruiz Multiobservational campaign GW170817/SSS17a. J. Astrophys., 870(2), L43.

Miller, A., Lin, K., Shen, H., George, D., and others. (2018). gravity wave detection with deep filtering. 103021 in Physical Review D, 97(10).

Mooley, K. P., Hallinan, G., Corsi, A., Nakar, E., and others. (2019). The sister of GW170817 by radio. Science 358, no. 6370 (2002), pp 15791583.

LaBolle, T., AmaroSeoane, P., Abernathy, M., Acernese, F., et al. (2019). Einstein Telescope design study. LIGO Scientific Collaboration et al. 2019. Classical and Quantum Gravity 27 (19) 194101. The impact of GW170817 on the gravity theories. Physical Review Vol. 123, No. 1, letter, 011102.

Virgo Collaboration, LIGO Scientific Collaboration (2020). There are limits to Hubble constant on various messengers. Letters of Astrophysical Journal, August 29, 898(2), L39.

Cooperation Virgo - LIGO. (2020). The discovery of a massive object: an intermediate-mass black hole (GW190521). Letters on Physical Reviews, 125 (10), 101102.

Dao, P., Lopez Ariste, A., Sanchez, F., etc. (2020). The impacts of GW190521 on the gap of black hole masses. RAS; 497(3), 3216-3225].

Vitale, S., Essick, R., Lynch, R., et al. (2020). Auger: 2019 results, the gravity wave astronomy burst sources. 024041, Physical Review D, 101(2).

M., Zanolin and A. Mezzacappa (2019). bursts of gravitational waves produced by supernovae with core collapse. J Astrophys, 874, L1.

Abernathy, M., Acernese, F., Punturo, M., etc. (2019). The Einstein Telescope is a third-generation observatory.

Yokoyama, S., Tanaka, T., Suyama, T., and Sasaki, M. (2018). Princess in gravitational-wave astronomy. Physical Review Letters, 117(6), 0611012020.

Troja, E., van Eerten, H., Piro, L., and others. (2017). The GW170817 X -ray analog. 7174 in Nature, 557(7702).

Kocsis, B., Loeb, A., Haiman, Z., & Yunes, N. (2020). Physical Review D, 81, 123553 (2010); EMRIs EMRIs and Sgr. A*.